

## CHAPTER 4

### RESULTS AND DISCUSSION

#### 4.1 Morphology of the Toner Particles

The toner used in this research work is a mono-component toner. Investigation of toner shape was made using the Scanning Electron Micrograph (SEM), ISM-5410LV. The mean particle size is about 11.25  $\mu\text{m}$ . The enlarged electron micrograph of toner particles is shown in Figure 4-1. Obviously, the toner particles are irregular in shape.

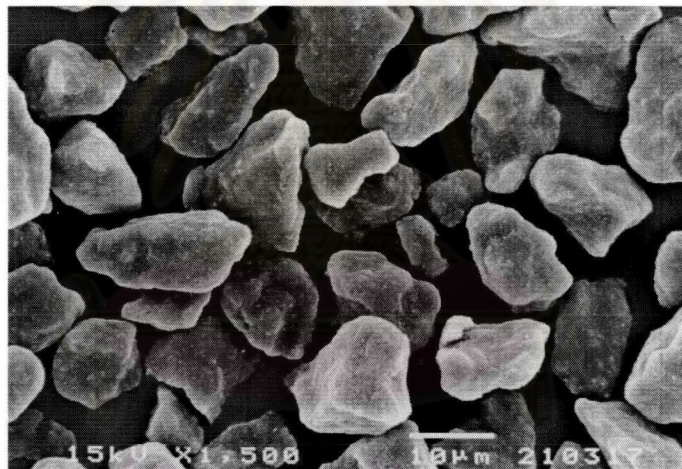


Figure 4-1 Scanning Electron Micrograph (SEM) of the toner particles showing the irregular shape of toner particles

#### 4.2 Determination of the Threshold Voltage

As mentioned in Chapter 3, one type of the toner used in this research work is conductive powders, which produce electrostatic induction within the particles. The specific gravity and the resistivity of toner are obtained from the manufacturer. The specific gravity  $\rho$  is  $1.9 \text{ g/cm}^3$  and the resistivity  $\eta$  is  $1.55 \times 10^{10} \Omega \text{ cm}$ .

To determine the threshold  $V_{th}$  of this toner, the experimental work for toner jumping is setup as described in Section 2.1.5 a). The amount of toner of about 1 mg is applied on the surface of the lower electrode. Then the voltage is applied to the electrodes. The current through the parallel plates is measured with a precision electrometer and is recorded as a function of applied voltage. The result is presented in Table 4-1.

Table 4-1 Applied voltage versus current measured between the parallel plates

Voltage (V)	Current (mA)
0	0.000
100	0.000
200	0.007
300	0.079
400	0.357
500	0.653
600	0.858
700	1.240
800	2.798
900	3.598
1000	4.356

The relationship between the applied voltage and the current flow through the parallel plates is accomplished as shown in Figure 4-2.

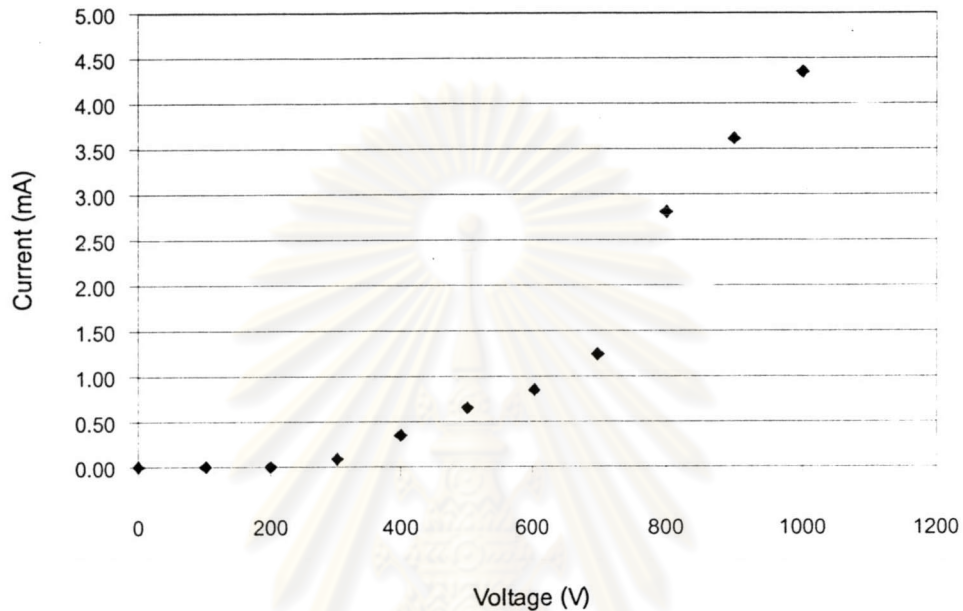


Figure 4-2 Determination of the threshold voltage

The analysis of the electrostatic current and voltage predicts the outcome when potential is applied to conductive materials which results in a voltage and current distribution over the surface of an object and its surrounding. In this case, the toner is conductive material and some of the electrons from their atoms can move freely throughout the material structure. When the voltage is applied to the pair of parallel plates, the conductive toner particles on the lower electrode become inductively charged due to the electric field between the electrodes. The induced charge particles will start jumping from the lower electrode to the upper electrode when the electrical field force overcomes the summation of gravitational force and the adhesion force between the toner particles and the substrate. In this case, an increasing magnitude of the current can be measured through the parallel plates. From the curve in Figure 4-2,

we can determine the applied voltage at which the toner particles start jumping,  $V_{th}$ . The threshold voltage  $V_{th}$  is about 300 Volts.

In consideration of charge quantity on the particle surface, the particles in the micrometer range are idealized to be spherical and effects of any molecular interaction or chemical reactions are neglected. It is assumed that the charge is distributed homogeneously on the surface.

For a conductive spherical particle, the acquisition of the induction charge resides on the surface of the particle and is nearly instantaneous. The total induced charge  $Q$  can be calculated as follows.<sup>10</sup>

$$Q = 1.65 \times 4\pi\epsilon_0 r^2 E_{th} \quad (4.1)$$

where  $r$  is the radius of the particle,  $\epsilon_0$  is dielectric constant of the free space and  $E_{th}$  is electric field when  $V_{th}$  is applied.

Since the electric field is uniform between two parallel plates, the electric field strength  $E_{th}$  can be calculated as follows.

$$E_{th} = \frac{V_{th}}{d} \quad (4.2)$$

where  $V_{th}$  is the threshold voltage and  $d$  is a distance between the parallel plates. The magnitude of each parameter is presented as follows.

$$V_{th} = 300 \text{ V}$$

$$d = 0.5 \text{ mm}$$

$$r = \frac{11.25}{2} \mu\text{m}$$

$$\epsilon_0 = 8.85 \times 10^{-12} \frac{\text{C}^2}{\text{Nm}^2} \quad (4.3)$$



Then the quantity of induced charge becomes  $3.5 \times 10^{-15}$  C. This means that the total charge on toner particle before separating from the lower electrode is about  $-3.5 \times 10^{-15}$  C.

#### 4.3 Toner Dot Confirmation

To confirm the generation of a toner dot, the TCB experiment was first setup. The amount of conductive toner of about 1 mg is applied on the surface of dented electrode.

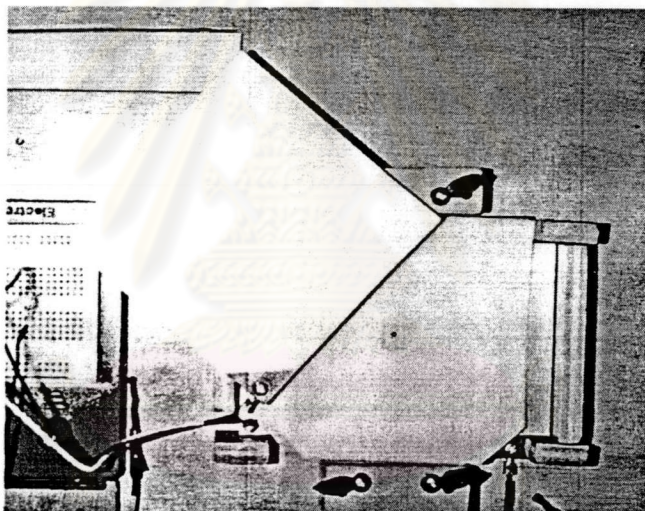


Figure 4-3 Toner dot confirmation

When more than a certain amount of voltage is applied between the electrodes, conductive toners move from the dented electrode and pass through the control electrodes until it reaches the paper that adhered beneath the pulling electrode. Because the toners are charged by conduction from the dented electrode under the electric field applied and the electric force works on the toner particles. A toner dot is then generated on the paper as shown in Figure 4-3.

According to the experiment, the first toner dot is obtained at a condition of the applied voltage to the lower electrode is 600 V, and to the upper control electrode is 660 V. The toner dot obtained is shown in Figure 4-3. This is the confirmation that the toner dot is generated. The toner dot area is measured by Program Image-Pro PLUS version 4.0.0.11. The unit of a toner dot area is in squares of millimeter.

#### 4.4 Dependence of Toner Dot Size on Aperture Size

To elucidate the effect of aperture size of control electrode on the toner dot size, two sets of control electrodes are used in the TCB experiment. The aperture diameter of one set is about 1 mm while the other is about 2 mm.

The experiment is carried on with many applied voltages for each electrode. The adjustment of applied voltage is done by adjusting a series of resistors in the circuit as indicated in Figure 3-1. Since a total number of resistors are not changed, so the voltage at the pulling electrode is a constant value of 650 V. When adjusting the series of resistors in the circuit, the voltage at the upper control electrode and the lower control electrode are changed, which is equal the summation of the voltage drop across those numbers of resistors changing. The voltage applied to the upper control electrode is in range of 234-509 V, while the voltage applied to the lower control electrode is in range of 100-502 V.

The obtained toner dots are measured for the dot area by program Image-Pro PLUS version 4.0.0.11. The unit of the toner dot area is  $\text{mm}^2$ .

The results of 1 mm and 2 mm of aperture diameter are shown in Tables 4-2 and 4-3. The relationships between the applied voltage to the lower control electrode and the average dot area are shown in Figures 4-4 and 4-6. In the opposite way, the relationships between the applied voltage to the upper control electrode and the average dot area are shown in Figures 4-5 and 4-7. The solid lines are trend lines.

Table 4-2 Applied voltage versus dot area for diameter of the aperture of 1 mm

Applied Voltage (Volts)				Average dot area (mm <sup>2</sup> )
pulling electrode	upper control electrode	lower control electrode	dented electrode	
650	569	100	0	0.1719
650	569	167	0	0.2945
650	569	234	0	0.3957
650	569	301	0	0.5209
650	569	368	0	0.5798
650	569	435	0	0.5624
650	569	502	0	0.5276
650	502	100	0	0.1075
650	502	167	0	0.1927
650	502	234	0	0.3309
650	502	301	0	0.3681
650	502	368	0	0.3624
650	502	435	0	0.3086
650	435	100	0	0.0362
650	435	167	0	0.1456
650	435	234	0	0.3026
650	435	301	0	0.364
650	435	368	0	0.331
650	368	100	0	0.0072
650	368	167	0	0.0573
650	368	234	0	0.2234
650	368	301	0	0.2711
650	301	100	0	0.0072
650	301	167	0	0.0525
650	301	234	0	0.2134
650	234	100	0	(no dot)
650	234	167	0	0.0504
650	167	100	0	(no dot)



Table 4-3 Applied voltage versus dot area for diameter of the aperture of 2 mm

Applied Voltage (Volts)				Average dot area (mm <sup>2</sup> )
pulling electrode	upper control electrode	lower control electrode	dented electrode	
650	569	100	0	1.0446
650	569	167	0	1.2973
650	569	234	0	1.5827
650	569	301	0	1.7706
650	569	368	0	1.7195
650	569	435	0	1.6600
650	569	502	0	1.5354
650	502	100	0	0.9862
650	502	167	0	1.2565
650	502	234	0	1.4502
650	502	301	0	1.6482
650	502	368	0	1.6459
650	502	435	0	1.4829
650	435	100	0	0.8502
650	435	167	0	1.2039
650	435	234	0	1.3934
650	435	301	0	1.6364
650	435	368	0	1.5432
650	368	100	0	0.7554
650	368	167	0	0.9193
650	368	234	0	1.3222
650	368	301	0	1.3880
650	301	100	0	0.6503
650	301	167	0	0.9497
650	301	234	0	1.0255
650	234	100	0	0.4456
650	234	167	0	0.6063
650	167	100	0	0.1242



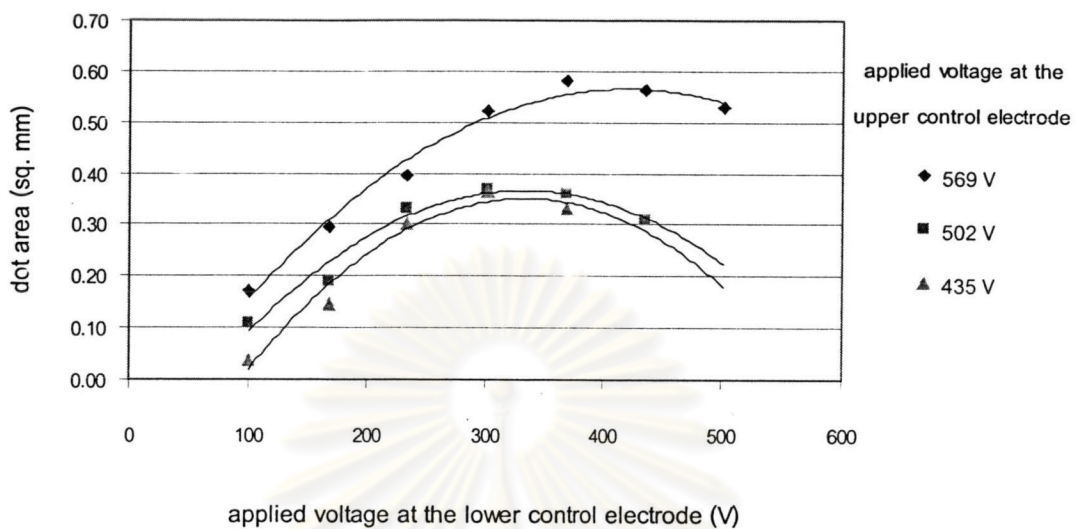


Figure 4-4 Applied voltage at the lower control electrode versus dot area for diameter of aperture of 1 mm

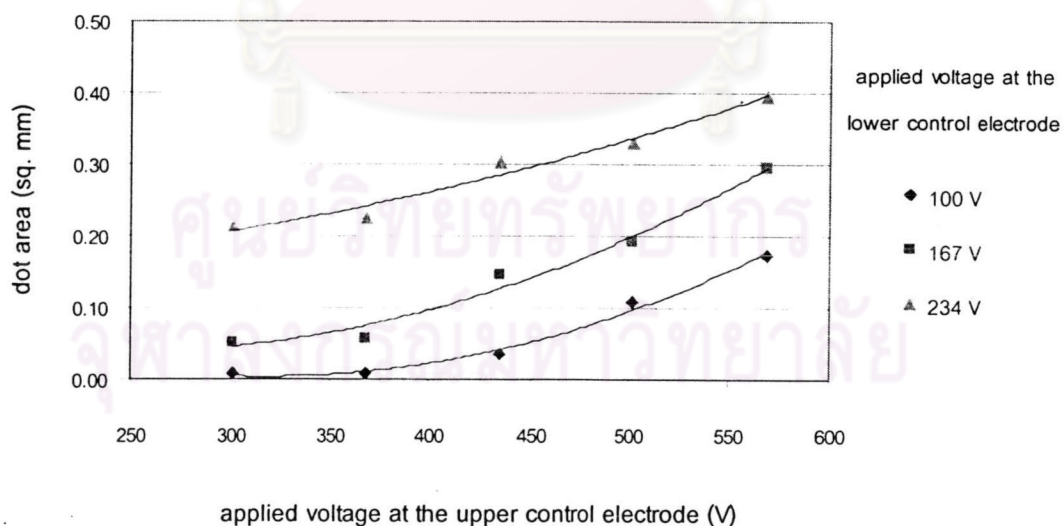


Figure 4-5 Applied voltage at the upper control electrode versus dot area for diameter of aperture of 1 mm

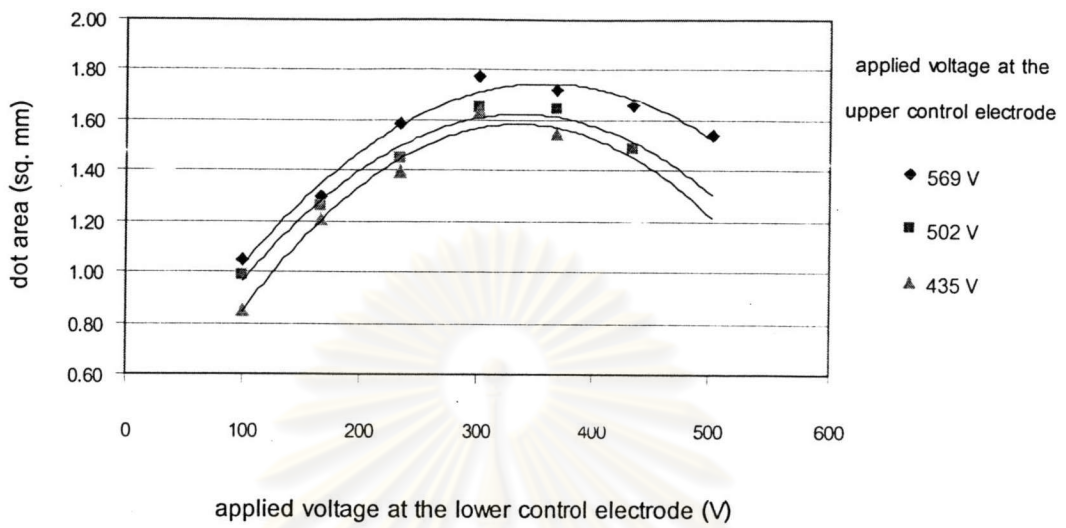


Figure 4-6 Applied voltage at the lower control electrode versus dot area for diameter of aperture of 2 mm

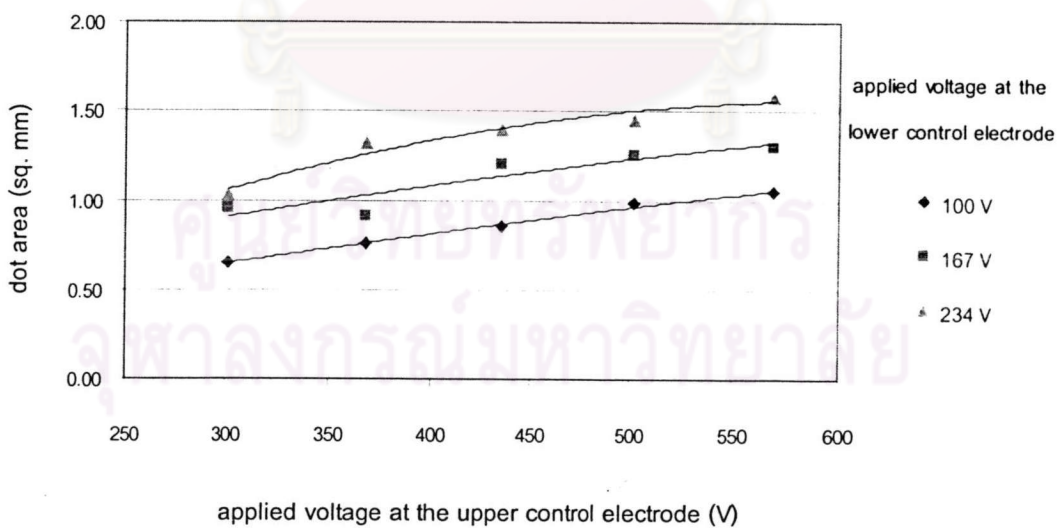


Figure 4-7 Applied voltage at the upper control electrode versus dot area for diameter of aperture of 2 mm

According to Figures 4-4 and 4-6, the toner dot size is increasing when the applied voltages at the lower control electrode is in an increasing range 0 to 300 V. When the applied voltage is increased further, the toner dot size tends to decrease. This result coincides with Section 4.2 in that the toner particles between the parallel plates start to jump at the applied voltage to the upper plate at about 300 V. When the applied voltage at the lower control electrode continues to increase, the potential difference between the lower control electrode and the upper control electrode decreases and reduces the toner dot size. Moreover, the curves indicate that when the applied voltage to the upper control electrode is 569 V, the toner dots are bigger than those caused by the applied voltage of 502, and 435 V, respectively. Because of an increasing in applied voltage at the upper control electrode contributes the potential difference between the upper control electrode and the lower control electrode to increase.

In Figures 4-4 and 4-6, when the applied voltage at the lower electrode is fixed, the toner dot increases by adding more applied voltage at the upper control electrode. This observation can be realized only when the applied voltage at upper control electrode is at 300 V or higher. Whenever the applied voltage to the upper control electrode is less than 300 V, a toner dot can not be obtained. Logically, the applied voltage to the lower control electrode at 234 V generates the bigger toner dots than the applied voltage at 167, and 100 V, respectively.

Although the toner dot size as described above are in a similar tendency, when the control electrodes of about 1 and 2 mm in the aperture diameter are applied, the size of a toner dots is different. As presented in Figures 4-8 to 4-13, a toner dot size created by 2 mm in aperture diameter of the control electrodes is bigger than a dot created by 1 mm in aperture diameter.

When the slopes of the curves in Figures 4-8 to 4-10 are considered, the applied voltage to the lower control electrode increase at a constant rate, a toner dot created by 2 mm aperture diameter is greater than that created by 1 mm. This

observation is also noted when the applied voltage to the upper control electrode is increase at a constant rate as shown in Figures 4-11 to 4-13.

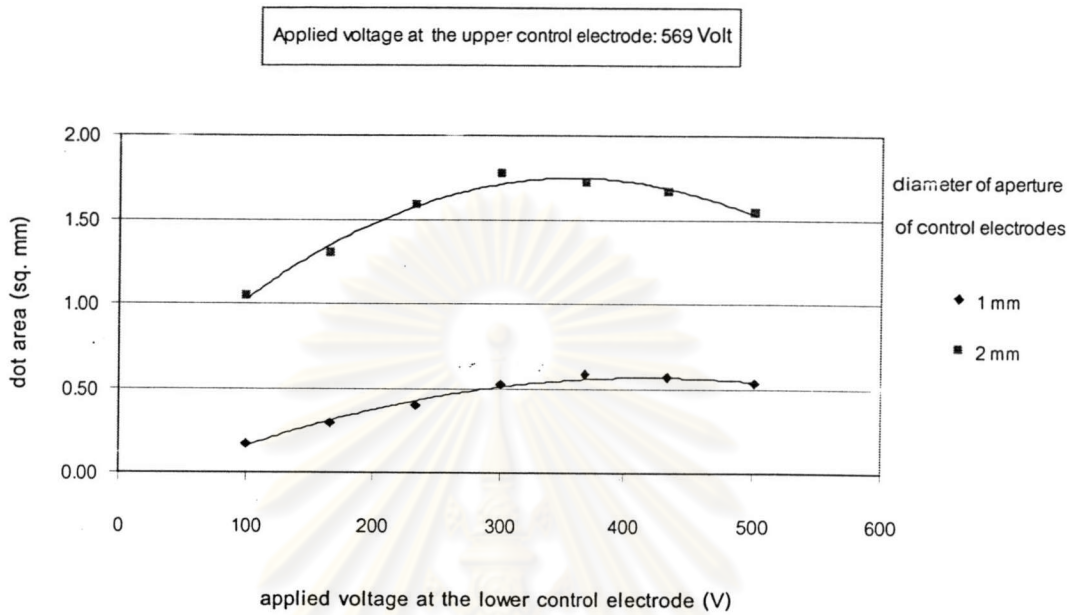


Figure 4-8 Applied voltage at the lower control electrode versus dot area for the applied voltage at the upper control electrode of 569 V

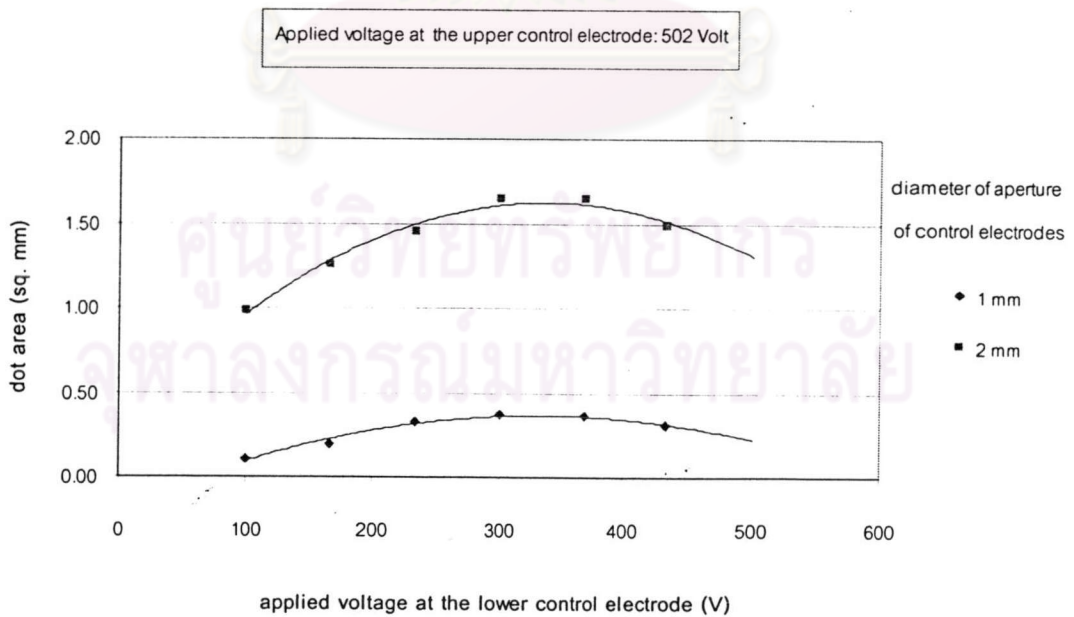


Figure 4-9 Applied voltage at the lower control electrode versus dot area for the applied voltage at the upper control electrode of 502 V



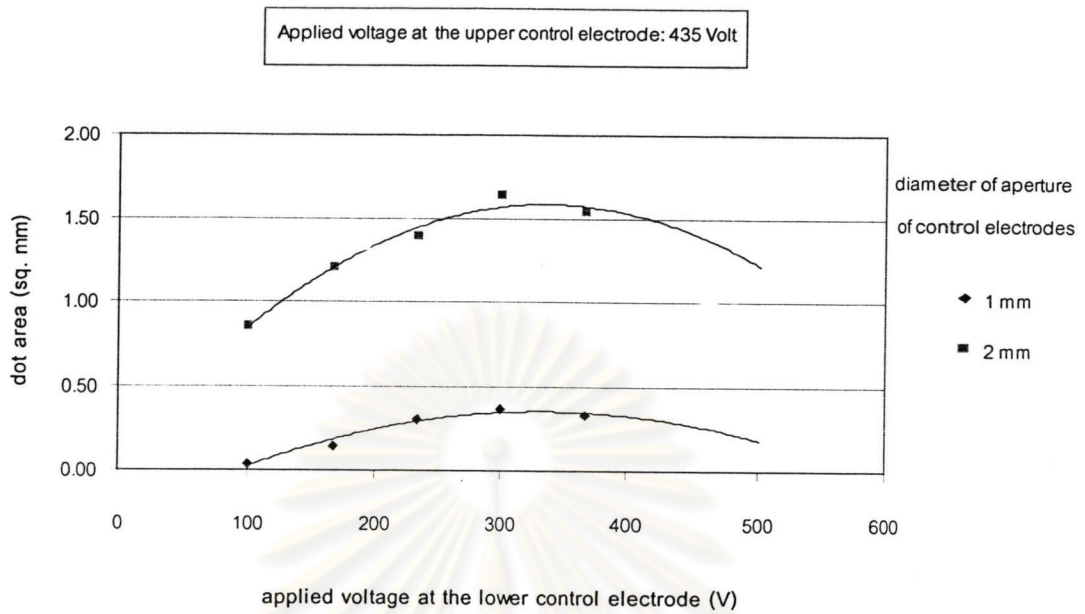


Figure 4-10 Applied voltage at the lower control electrode versus dot area for the applied voltage at the upper control electrode of 435 V

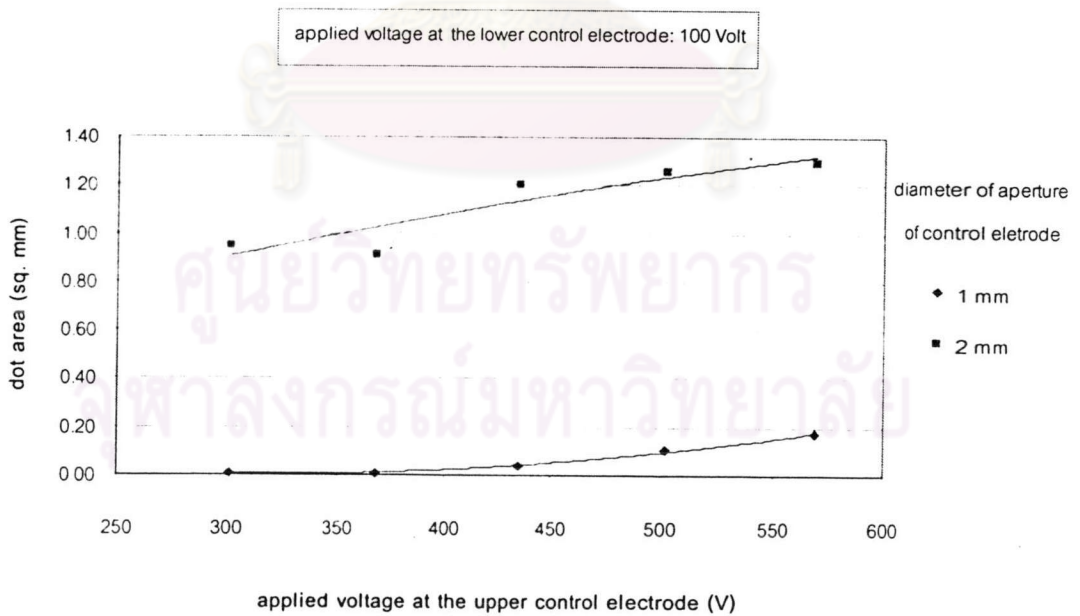


Figure 4-11 Applied voltage at the upper control electrode versus dot area for the applied voltage at the lower control electrode of 100 V

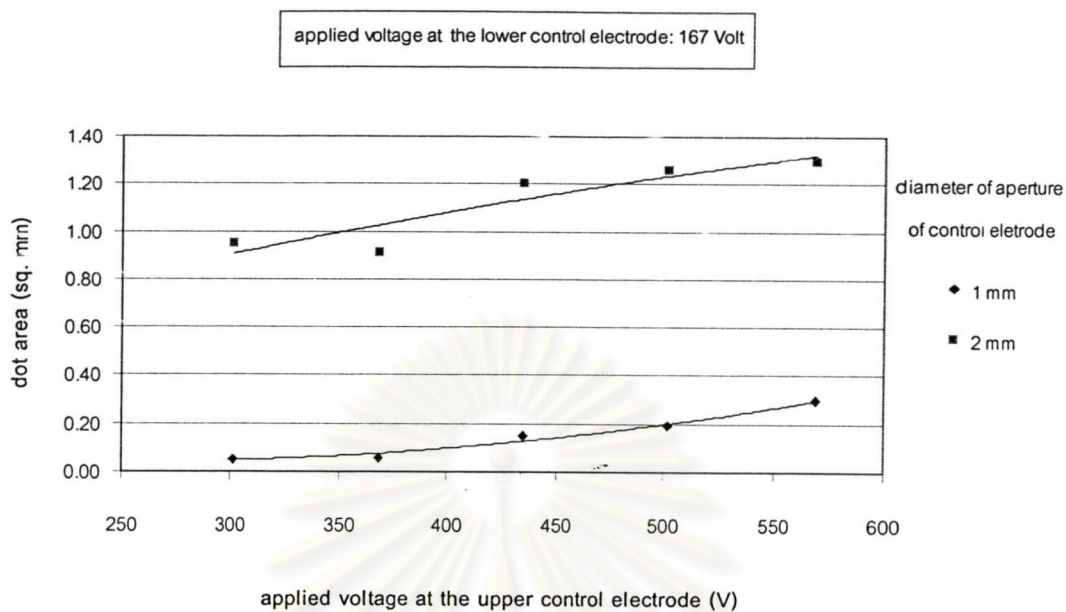


Figure 4-12 Applied voltage at the upper control electrode versus dot area for the applied voltage at the lower control electrode of 167 V

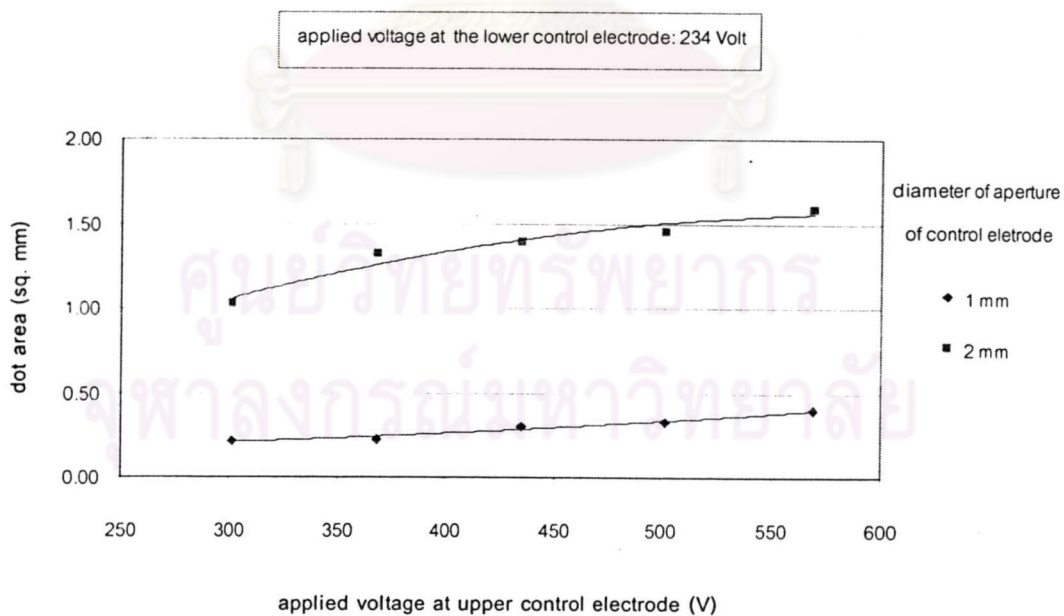


Figure 4-13 Applied voltage at the upper control electrode versus dot area for the applied voltage at the lower control electrode of 234 V

#### 4.5 Dependence of Toner Dot Size on Applied Voltage

In this investigation, the applied voltage is given to a higher value than those in Section 4.4. In addition, the applied voltage to the pulling electrode is not fixed as previously, and the different potentials are wider in the range of hundred volts. The control electrodes used in the experiment have the aperture diameters of 0.5 and 0.8 mm.

The experiment starts with by the control electrodes with 0.5 mm in aperture diameter. The schematic layout of the applied voltage to the electrodes is shown in Figure 4-14, and various applied voltages given are shown in Table 4-3.

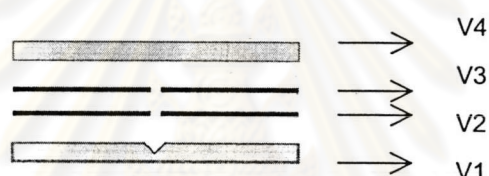


Figure 4-14 The schematic layout of the applied voltage to the electrodes in TCB

As shown in Table 4-4, the different potential between the dented electrode and the lower control electrode is fixed at 300 V ( $V_2 - V_1 = 300V$ ), and the different potential between the upper control electrode and the pulling electrode is fixed at 200 V ( $V_4 - V_3 = 200V$ ). The different potential between the upper control electrode and the lower control electrode is designed to vary from -150 V to 100 V.

The relationship between the toner dot size and the different potential  $V_3 - V_2$  is presented in Figure 4-15. According to the curve in Figure 4-15, the toner dot size tends to increase when  $V_3 - V_2$  is increased. This means that the distribution of electric field between the control electrodes affects the toner dot size. The experiment is continued by placing a new control electrode with an aperture diameter of 0.8 mm. The different

potential V4-V3 is varied for four values (100, 150, 200, and 300 V) as shown in Tables 4-5 to 4-8.

Table 4-4 Applied voltages for the aperture diameter of 0.5 mm at V4-V3=200V

Pulling electrode	Applied Voltage (Volt)			V3-V2 (Volt)
	upper control electrode	lower control electrode	dented electrode	
350	150	300	0	-150
400	200	300	0	-100
450	250	300	0	-50
500	300	300	0	0
550	350	300	0	50
600	400	300	0	100

Applied voltage versus average dot area (V4-V3=200 Volt)

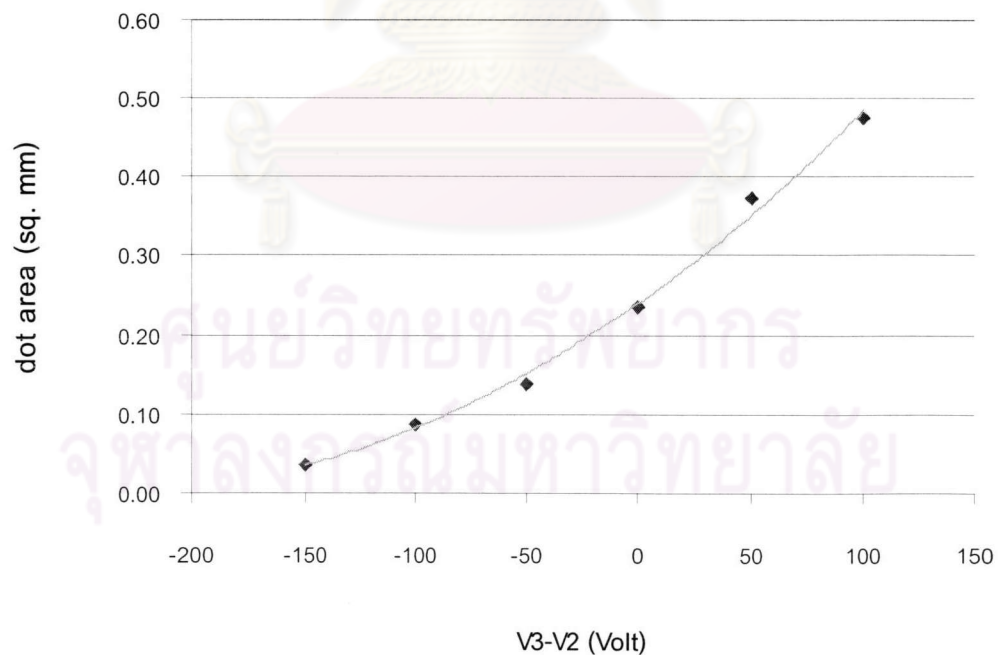


Figure 4-15 V3-V2 versus dot area for the aperture diameter of 0.5 mm at V4-V3=200 V



Table 4-5 Applied voltages for the aperture diameter of 0.8 mm at  $V_4-V_3=100V$ 

Applied Voltage (Volt)				V3-V2 (Volt)
Pulling electrode	upper control electrode	lower control electrode	dented electrode	
300	200	300	0	-100
350	250	300	0	-50
400	300	300	0	0
450	350	300	0	50
500	400	300	0	100

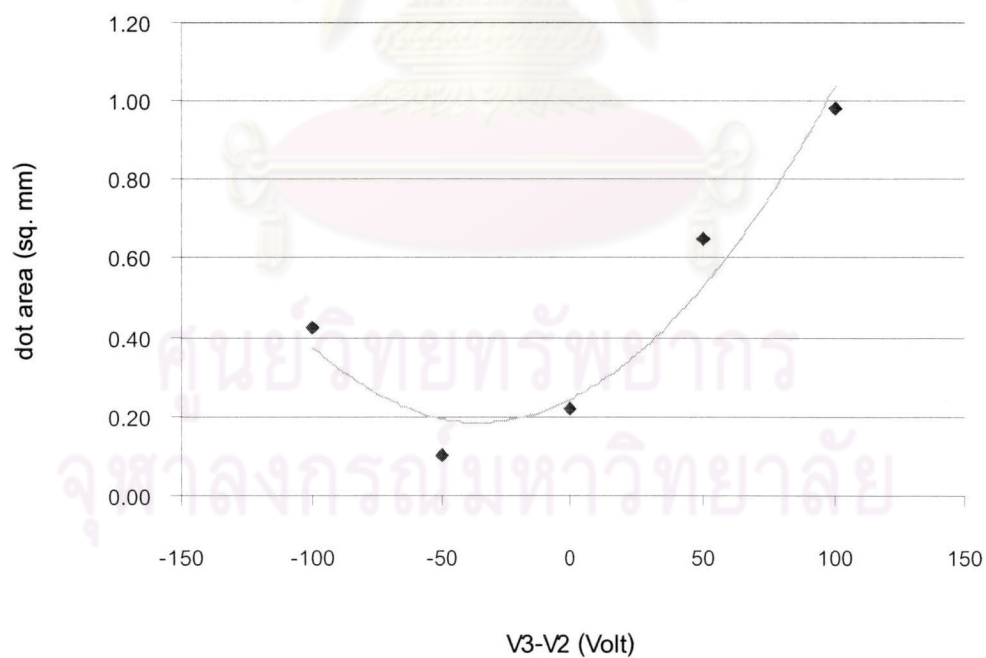
Applied voltage versus average dot area ( $V_4-V_3=100$  Volt)

Figure 4-16 V3-V2 versus dot area for the aperture diameter of 0.8 mm at

 $V_4-V_3=100$  V

Table 4-6 Applied voltages for the aperture diameter of 0.8 mm at  $V_4-V_3=150V$ 

Applied Voltage (Volt)				V3-V2 (Volt)
Pulling electrode	upper control electrode	lower control electrode	dented electrode	
350	200	300	0	-100
400	250	300	0	-50
450	300	300	0	0
500	350	300	0	50
550	400	300	0	100

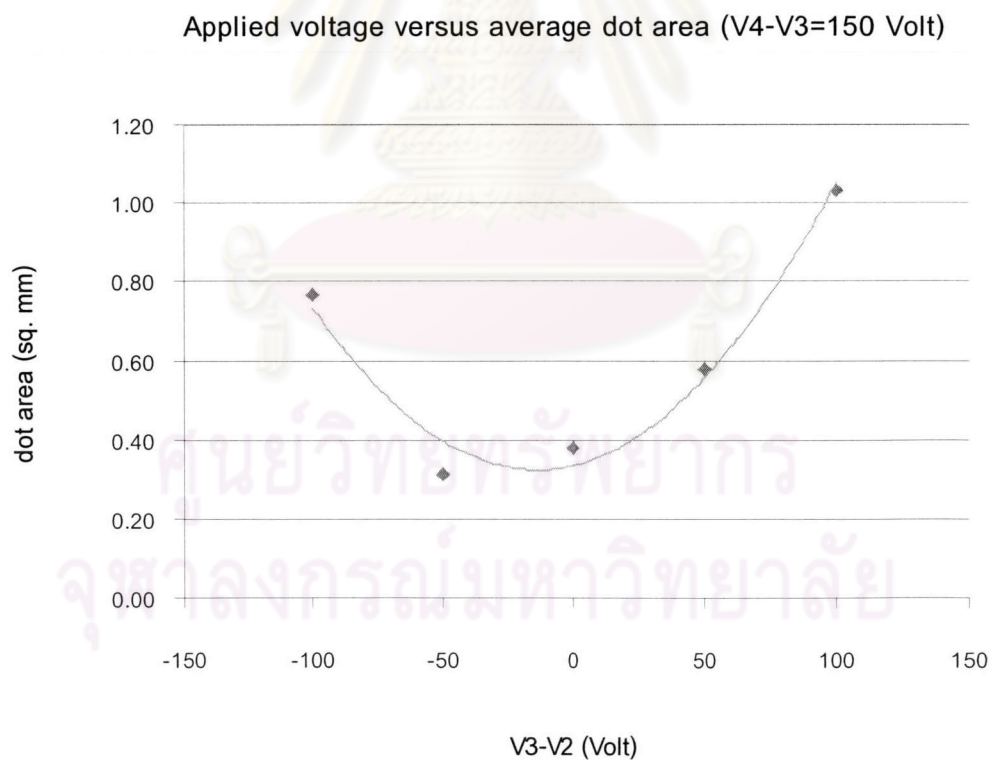


Figure 4-17 V3-V2 versus dot area for the aperture diameter of 0.8 mm at  
 $V_4-V_3=150$  V

Table 4-7 Applied voltages for the aperture diameter of 0.8 mm at V4-V3=200V

Applied Voltage (Volt)				V3-V2 (Volt)
Pulling electrode	upper control electrode	lower control electrode	dented electrode	
350	150	300	0	-150
400	200	300	0	-100
450	250	300	0	-50
500	300	300	0	0
550	350	300	0	50
600	400	300	0	100

Applied voltage versus average dot area (V4-V3=200 Volt)

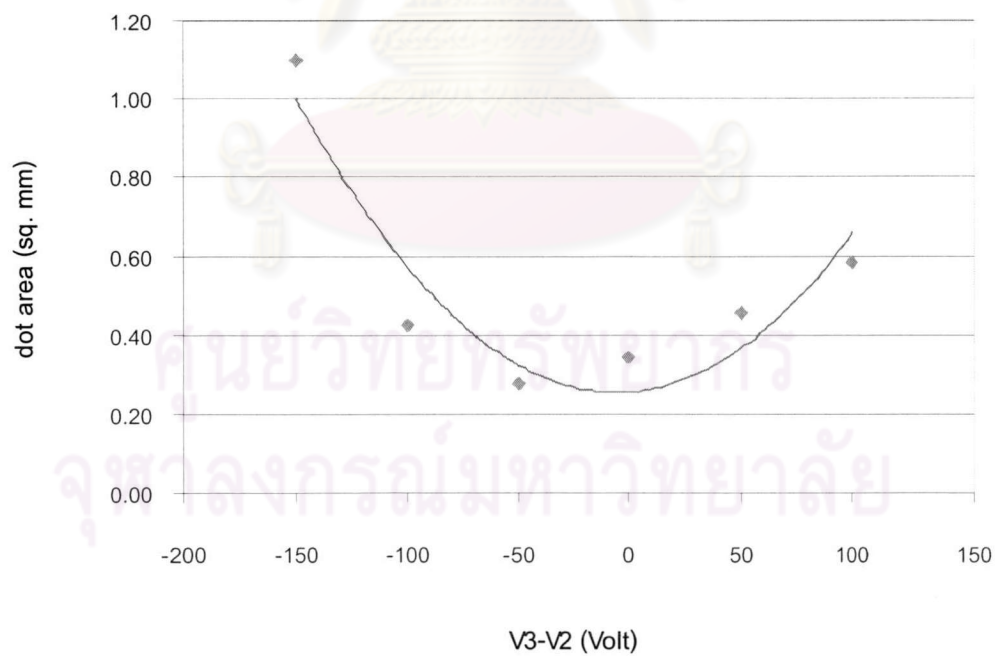


Figure 4-18 V3-V2 versus dot area for the aperture diameter of 0.8 mm at  
V4-V3=200 V

Table 4-8 Applied voltages for the aperture diameter of 0.8 mm at  $V_4-V_3=300V$ 

Applied Voltage (Volt)				V3-V2 (Volt)
pulling Electrode	upper control electrode	lower control electrode	dented electrode	
400	100	300	0	-200
500	200	300	0	-100
600	300	300	0	0
700	400	300	0	100

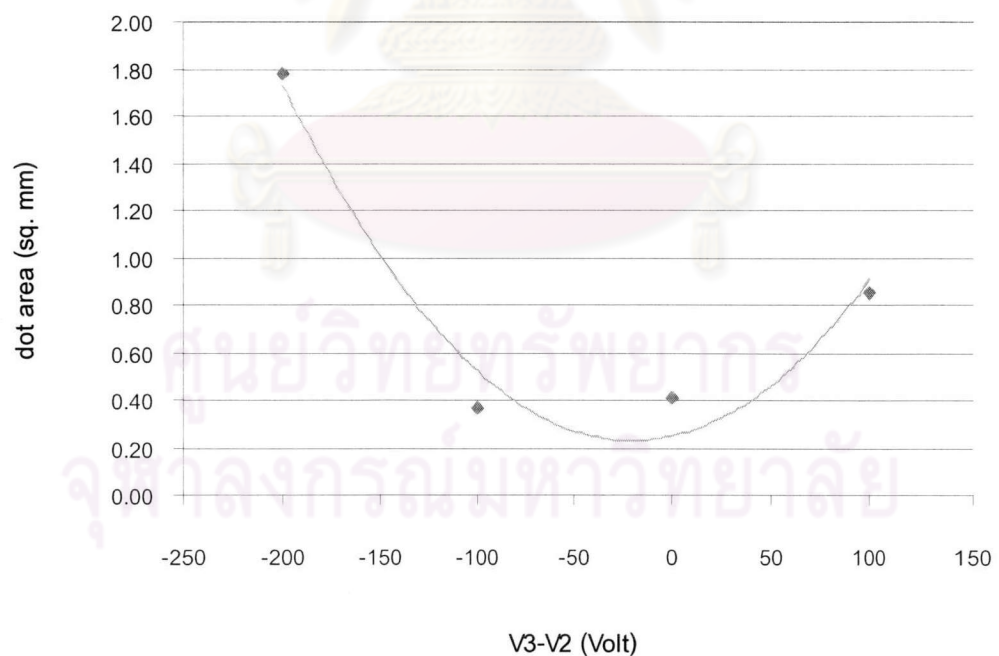
Applied voltage versus average dot area ( $V_4-V_3=300$  Volt)

Figure 4-19 V3-V2 versus dot area for the aperture diameter of 0.8 mm at  
 $V_4-V_3=300$  V



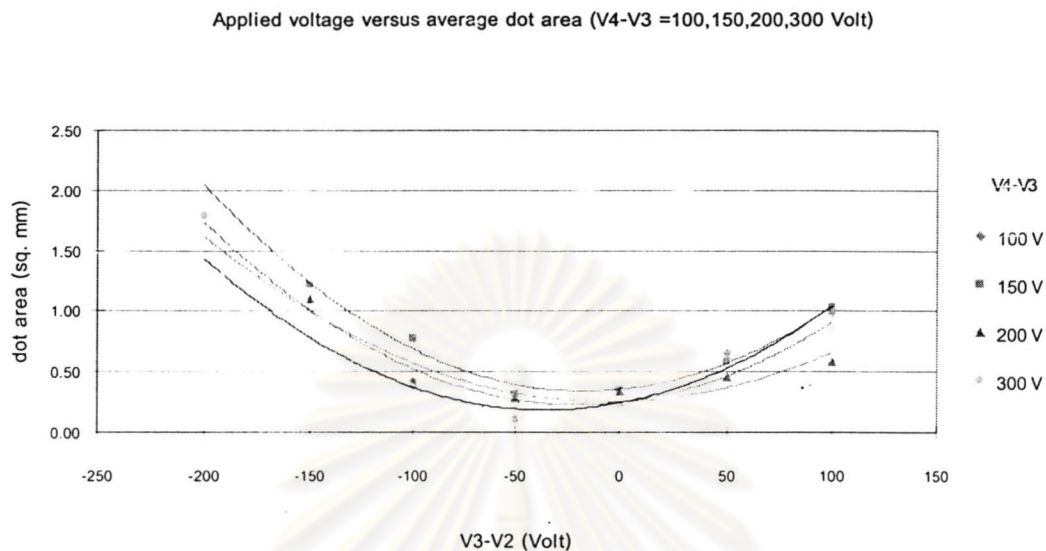


Figure 4-20  $V_3-V_2$  versus average dot area for the aperture diameter of 0.8 mm at  $V_4-V_3=100, 150, 200, 300$  V

When the control electrodes having the aperture diameter of 0.8 mm are used, the different potentials between the upper control electrode and the pulling electrode ( $V_4-V_3$ ) are fixed at four constant values of 100, 150, 200 and 300 V. The results are shown in Figures 4-16 to 4-19, respectively.

The resulting curves shown in Figures 4-16 to 4-19 are similar. Three regions are considered. The first region is the start at the different potentials between the upper and lower control electrode ( $V_3-V_2$ ), in the range  $-200$  V to  $-50$  V, the toner dot size is decrease and then reaches the minimum point, considered as the second region, which is in the range of  $-50$  V to  $0$  V. The third region is indicated at a range of  $0$  V to  $100$  V, the toner dot size tends to gradually increase. Figure 4-16 to 4-20 concludes the four different  $V_4-V_3$  values for comparison.

#### 4.6 Electric Field Analysis

The electric field components are calculated by software ELFIN (mini) version 5.02, which is an electrostatic field modeling program based on Integral Element Method (IEM). The feature of ELFIN is presented in Appendix B. In ELFIN (mini) consists of ELF series as follows:

- ELF/BEAM version 2.26
- ELF/MESH version 3.33

Referring to the calculation of electric field, the calculation procedures need ELFIN/MESH. The ELF/BEAM is also necessary when the toner trajectory is calculated.

ELF/MESH is an interpreter to make a geometry file (\*.meg). The input file of ELF/MESH is MEI. The output files of ELF/MESH are MEG and MEO. ELF/MESH reads and executes data lines in MEI one after another.

At the beginning, the input file etest.mei is first developed to generate the elements and nodes of material and space. In TCB system, there are four electrodes, which consist of the dented electrode, lower control electrode, upper control electrode and pulling electrode. A number of electrodes is a plate element and has an axial symmetry. The feature of the axial symmetry is described in Appendix B.

Since the ELFIN can determine the symmetry conditions of system, it is convenient to build the model in only the xz-plane. The schematic setup of elements for the calculation of electric field is shown in Figure 4-21.

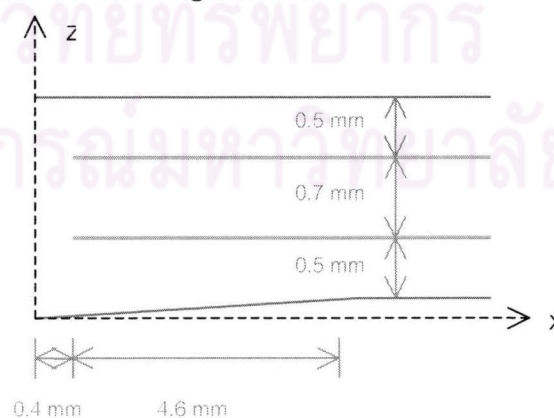


Figure 4-21 Schematic setup of elements for TCB system for the calculation of the electric field

Since the electric field between the parallel plates is the simplest case, and well known, so we begin to develop the program to calculate the electric field between parallel plates using ELFIN software. First, the elements and nodes of the parallel plates are created through etest.mei file. The result is shown in Figure 4-22.

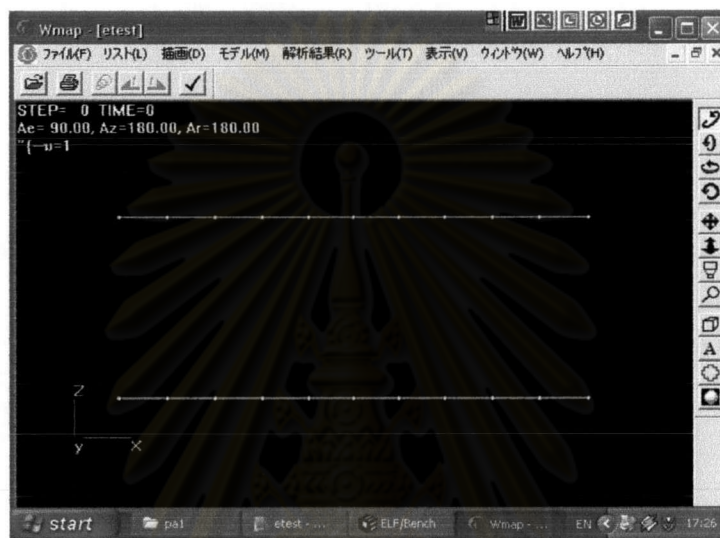


Figure 4-22 The elements and node of parallel plates created by ELFIN software

Then the elements and nodes of the space for electric field representation are created. This procedure is performed through etest.mei file too. The nodes at the space elements are corresponding to the values of electric field presented in etest.meo file. The number of nodes in space elements involves the accuracy of electric field calculation. If the number of nodes is increased, the outcome contains a small error. However, more nodes affect the increasing calculation time. The elements and nodes of the space between the parallel plates are shown in Figure 4-23. ELFIN unlike the conventional method such as FEM<sup>13-14</sup> in that it does not need the boundary condition to evaluate the physical quantities, electric field and electric force. ELFIN evaluates the electric field on the basis of Coulomb's law.

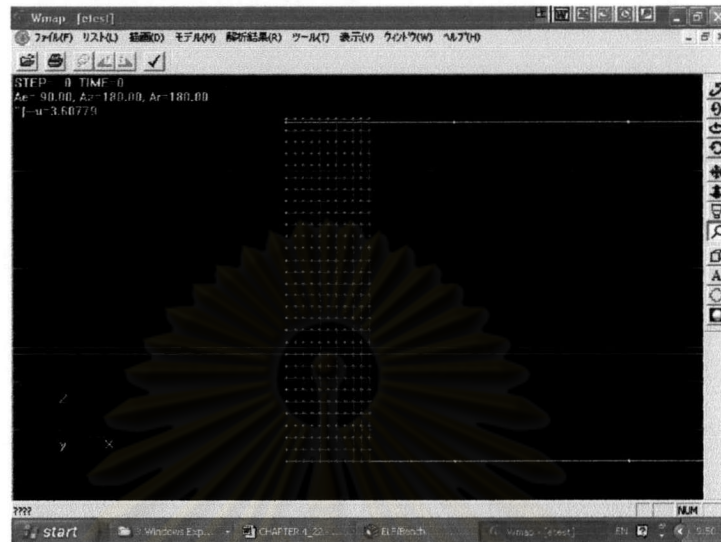


Figure 4-23 The space elements and nodes between parallel plates

Finally, the electric field is calculated through etest.mai file. In this procedure, the applied voltages at the material elements are defined through etest.mai file in order to calculate the electric field along the space elements. When the applied voltages to the parallel plates becomes as those in Figure 4-24, the appearance of electric field and equipotential curves are acquired as shown in Figure 4-25.



Figure 4-24 Condition of the applied voltage to the parallel plates



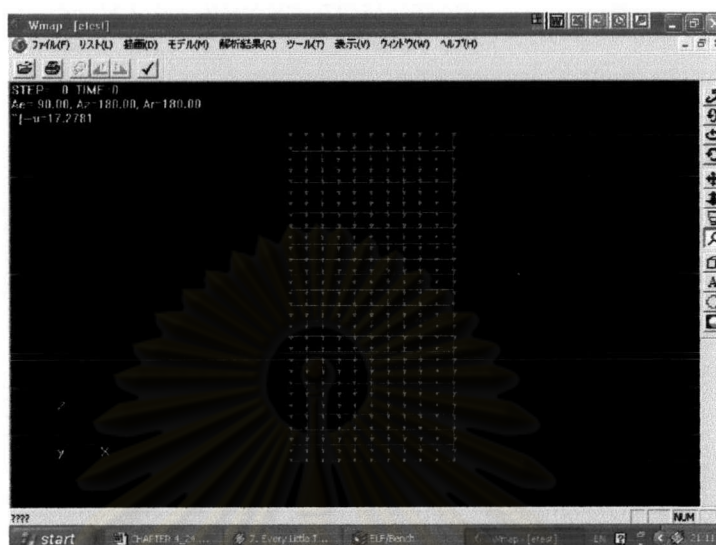


Figure 4-25 Electric field between the parallel plate calculated by ELFIN

In the diagram of Figure 4-24, the distance between the plates is 1.98 mm and the voltage across the plates is 300 V. The uniform electric field between the plates would be  $E = V / d = 300 \text{ V} / 1.98 \times 10^{-3} \text{ m} = 1.52 \times 10^5 \text{ V/m}$ . The solution of electric field between the parallel plates solved by ELFIN as shown in Figure 4.25 agrees with this value. Note that the value of electric field solved by ELFIN is little different from the analytical solution because ELFIN solves the electric field by including the effect of open end of the parallel plates.

Remember that, the direction of an electric field is defined as the direction that a positive test charge would move. So in this case, the electric field would point from the upper plate to the lower plate.

Next step, the electric field between the dented electrode and flat electrode is then calculated. According to the experiment, the dented electrode has a cone-shape surface with 10 mm in diameter and a depth of 0.2 mm at the center of the cone shape. Similarly to the parallel plates, the applied voltage is set at 0 V and 300 V. Figure 4-26

shows the schematic setup of the elements for electric field calculation, and the resulting electric field from ELFIN is shown in Figure 4-27.

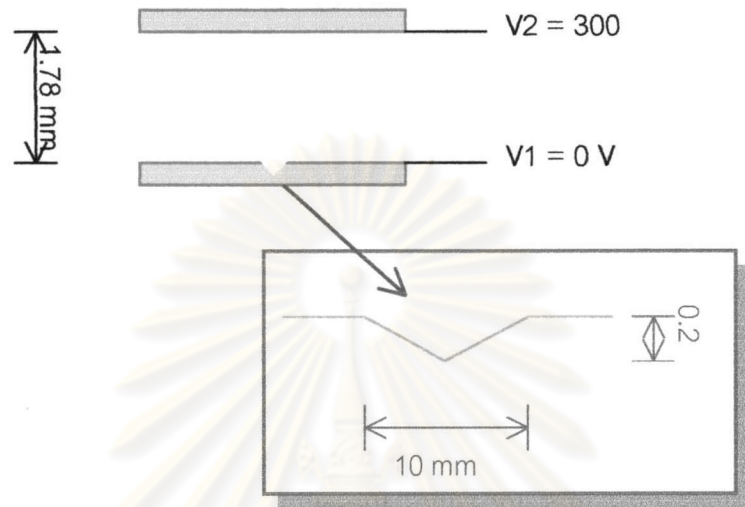


Figure 4-26 Experimental setup for simulation when the dented electrode is used

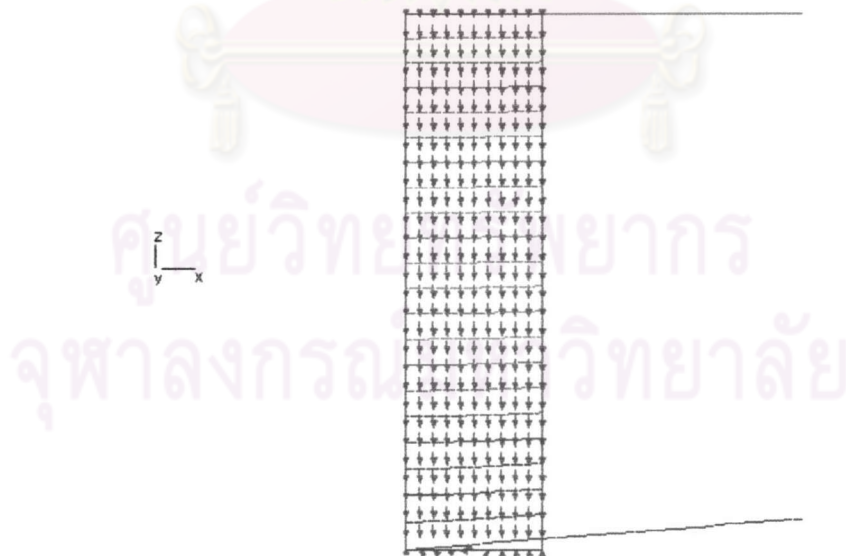


Figure 4-27 Equipotential contours and electric field streamlines between the dented electrode and flat electrode

Finally, the electric field of electrode used for TCB printing is calculated. As mentioned before, TCB consists of the dented electrode, upper control electrode, lower control electrode and pulling electrode placed parallelly. In this simulation, the aperture of the control electrodes is set at 0.8 mm in diameter and the control electrode is in the z axis at 0.4 mm when it is viewed in the xz plane. The voltage applied to a number of electrodes is set as shown in Figure 4-28. The result of the calculation is presented in Figure 4-29.

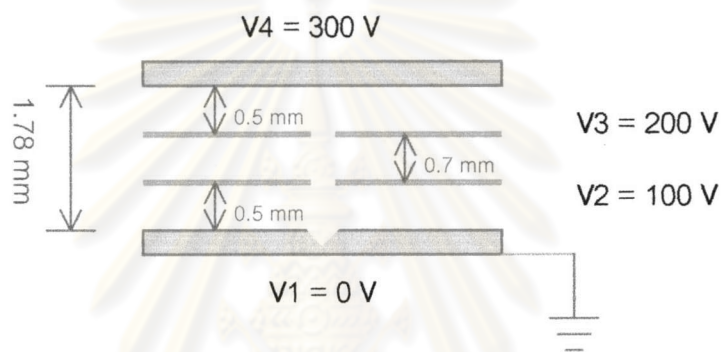


Figure 4-28 Experimental setup for simulation for a number of electrodes in TCB

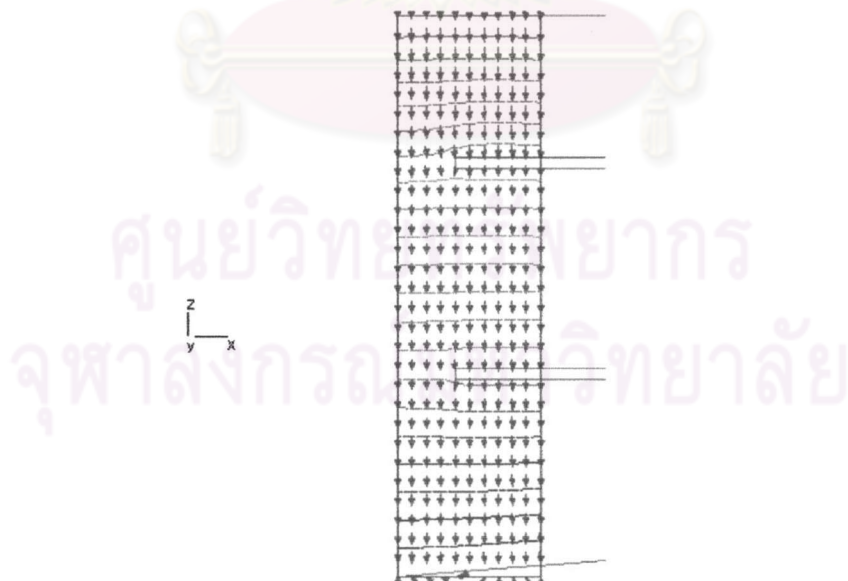
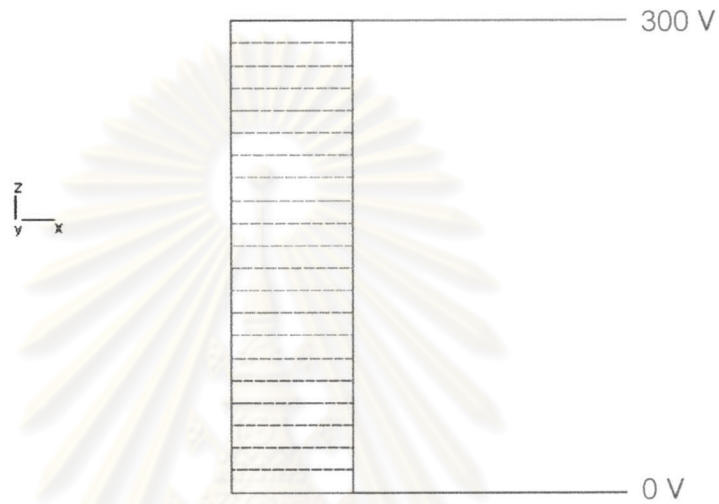
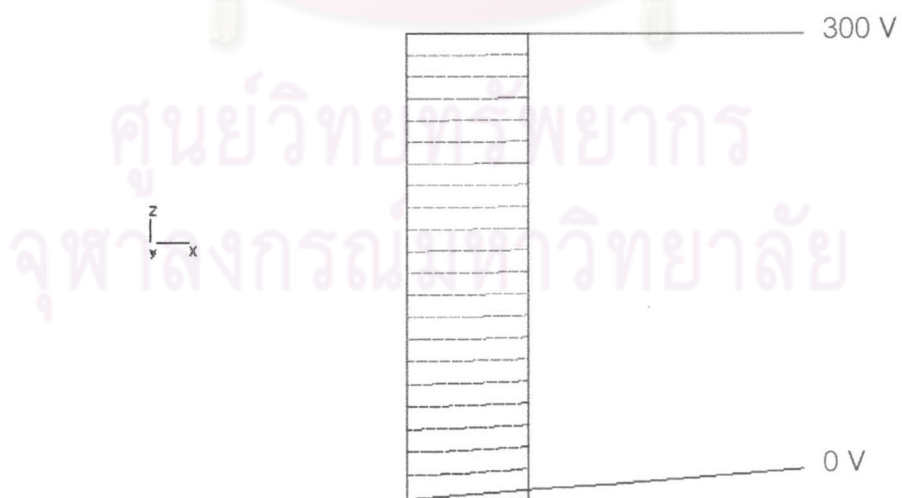


Figure 4-29 Equipotential contours and electric field streamlines between a number of electrodes setup in TCB

The equipotential contours are different for those kinds of element material. In Figure 4-30, the element material is desired to have a same distance of separate plates in the z axis and same applied voltage at upper plate. Then the results are compared as shown in Figure 4-30.



a) Parallel plates



b) Dented plate and flat plate



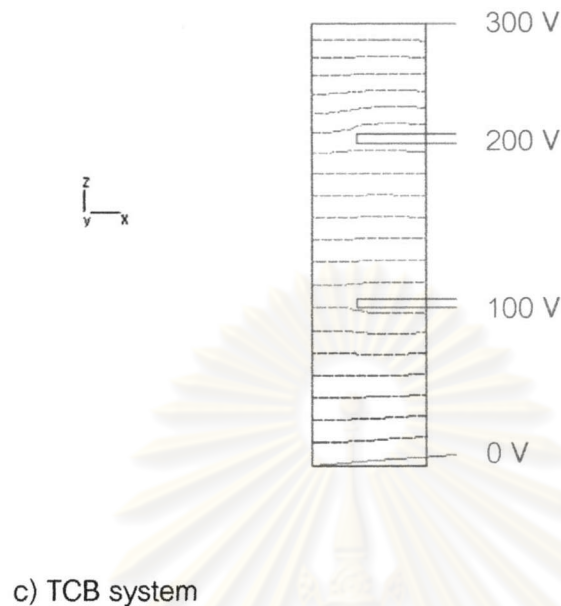


Figure 4-30 Comparison of equipotential contours for different element material

For a metallic conductor, the electric field is perpendicular to the surface, just outside a conductor, and therefore the direction of an electric field depends on the shape of the conductor. Then the direction of an electric field between two parallel flat plates would point straight from the upper plate to the lower plate and is perpendicular to the lower plate as shown in Figure 4-25. The equipotential contours of the parallel plates are parallel to the plates as shown in Figure 4-30 a). When the dented plate is applied, the direction of an electric field is curved to the central axis as shown in Figure 4-27. This indicates that the dented plate has been effectively confined to charged particles in the dented area because the electric field has the component in the  $x$  axis ( $E_x$ ) toward the  $z$  axis when compared with the parallel plates. The contour map of dented plate in two dimensions as shown in Figure 4-30 b) is obviously different from Figure 4-30 a). When inserting the control electrodes like that in the TCB system, the electric field and equipotential contours are changed as shown in Figures 4-29 and 4-30 c). This difference can be understood by a plot between the magnitude of electric field and the distance along the  $z$  axis as shown in Figure 4-29. The blue curve, pink curve,

and green curve show the magnitude of electric field of the parallel plates, the dented plate and the flat plate, and the TCB system, respectively.

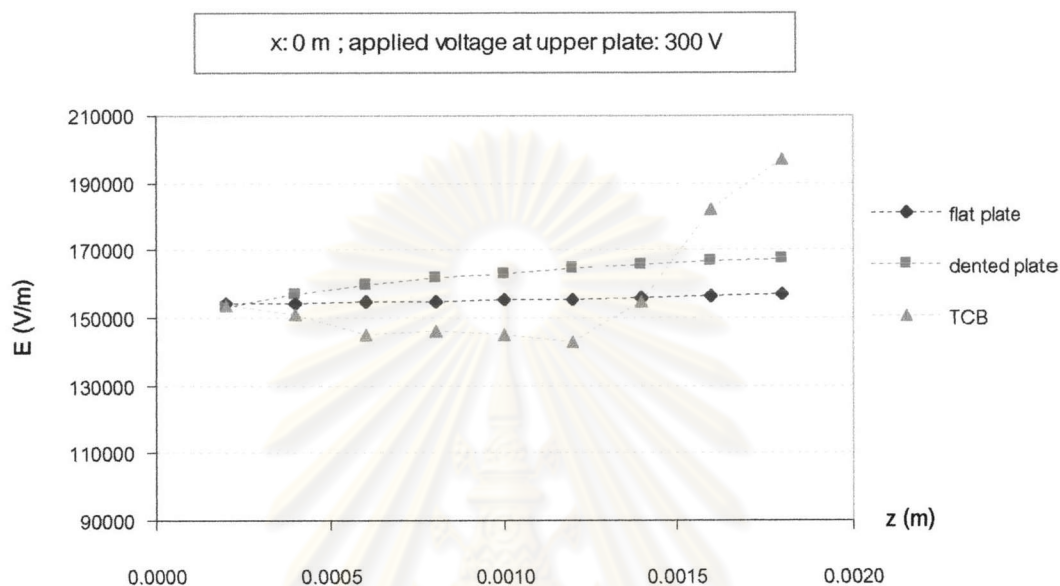
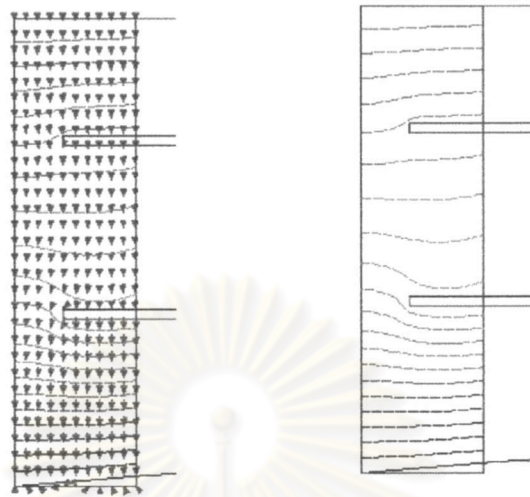


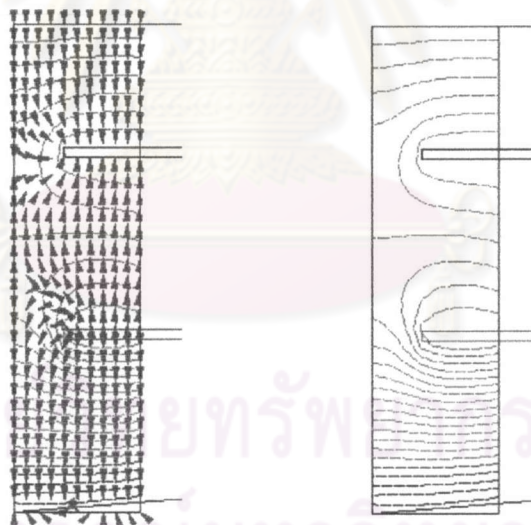
Figure 4-31 Electric fields versus distance along the z axis at the applied voltage of the upper plate of 300 V

One can view that when inserting the control electrode between the dented plated and the flat plate, the magnitude of electric field along the z axis become non uniform. The applied voltages at the control electrodes affect the magnitude of electric field along the z-axis. In this case, the applied voltages for TCB are 0, 100, 200 and 300 V. As shown in Figure 4-30 c), the direction of an electric field is downward to the dented electrode. Since an electric field force can be calculated by  $F = qE$ , so the negative charge in this field will move up to the pulling electrode.

Now we consider the effect of applied voltage to the control electrodes. Two different conditions are calculated by ELFIN, one is for 0, 300, 400, 500 V and the other is for 0, 300, 200, 300 V. Two of these conditions have  $V_2 - V_1 = 300$  V and  $V_4 - V_3$  of 100 V. The difference is that  $V_3 - V_2$  for the first condition is 100 V, while the other is -100 V. The results are shown in Figure 4-32.



a) Applied voltage of 0, 300, 400, 500



b) Applied voltage of 0, 300, 200, 300

Figure 4-32 Electric fields at different condition of applied voltage

When  $V_2 > V_3$ , the direction of an electric field between the upper control electrode and the lower control electrode is downward to the dented electrode as shown in Figure 4-32 a). Since an electric field force can be calculated by  $F = qE$ , so the negative charge in this field can move up from the lower control electrode to the upper control electrode.

Obviously in Figure 4-32 b), when  $V_2 < V_3$ , the electric field become pointing upwards to the pulling in the area between the upper control electrode and the lower control electrode. The field force acting on the negative charge is downward and can be a barrier for the movement of toner particles if the electric field in that area is strong enough.

The explanations above indicate that the dented electrode and the pulling electrode are used for confinement of the toner particles in the dented area and the control electrodes are inserted between the dented electrode and the pulling electrode for controlling an electric field contributed between the lower control electrode and upper control electrode, which affects the trajectories of the toner particles passing through this area.

#### 4.7 Toner Trajectory

When the electric fields are obtained, the trajectory of charged particles in these fields can be then calculated. In the TCB system, toner particles move from the dented electrode through the aperture of the control electrodes and reach the paper beneath the pulling electrode. The movement of the charge toner particles can be simulated using ELFIN/BEAM. ELFIN/BEAM uses the data of the electric field for calculations by ELFIN.

ELFIN/BEAM can calculate the toner trajectory with the equation of motion, as follows.

$$\vec{F} = m\vec{a} \quad (4.4)$$



From Equation (4.4), forces acting on the particles in the ELFIN/BEAM compose of electrical field force and air draught force.

The electrical field force,  $\vec{F}_e$ , is calculated from the electrical field and the charge of the particle as shown in Equation (4.5)

$$\vec{F}_e = Q\vec{E} \quad (4.5)$$

The electrical field components are calculated by the ELFIN software and the total induced charge is determined according to the method in Section 4.2. Note that the toner particles are irregular in shape as shown in the micrograph of Section 4.1. So the induced charge is not a uniform distribution on the surface of toner particles. However, when the simulation is preceded, we must assume that the toner particle is a spherical shape.

The air draught force acting on a spherical object under laminar flow is calculated from Stoke's theory which depend on the velocity of the moving particle

$$\vec{F}_a = 6\pi\eta r\vec{v} \quad (4.6)$$

where  $\eta$  is the coefficient of viscosity of air, which is  $1.81 \times 10^{-5}$  Pa s. The air draught becomes  $1.92 \times 10^{-9} \times$  velocity of the toner particle ( $v$ ).

Then the equation of motion becomes Equation (4.7)

$$\vec{F} = m\vec{a} = Q\vec{E} - k\vec{v} \quad (4.7)$$

where  $k = 1.92 \times 10^{-9}$  kg/s and  $m$  is the mass of toner particle, which can be describe as in Equation (4.8)

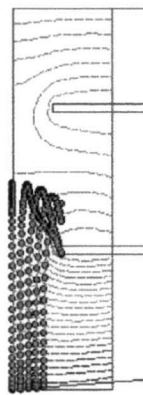
$$m = \frac{4}{3}\rho\pi r^3 = 1.42 \times 10^{-12} \text{ kg} \quad (4.8)$$

The number of toner particles, the initial position and the initial velocity of the toner particles are first set in `btest*mei`. Then the step time and space in the simulation is set in `btest.mai`. The values of  $m$ ,  $Q$  and  $k$  are also input into `btest.mai`.

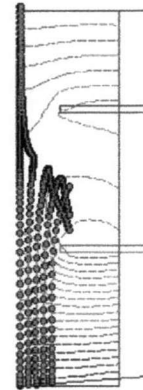
The particle trajectory has been solved numerically in a small-time step (0.1 ms) under 2 assumptions: 1) the effect of micro discharge is very small and can be thus neglected; 2) the charge on the particle change can only through contact with the electrode.

When we simulate five toner particles arranged on the dented electrode, the toner trajectories are obtained as shown in Figures 4-33 to 4-36. Each line represents the trajectory of a toner particle. Each point of each line represents the trajectory at intervals of 0.1 ms. The trajectories of toner particles depend on electric field force as described above, and therefore when the voltage applied to the electrodes are change, the trajectories are changed. To compare between the experiment and the simulation, the trajectories of five toner particles has been simulated using the value of applied voltage corresponding to the experiment. The conditions of applied voltage are shown in Tables 4-5 to 4-8 of Section 4.5. These simulations of toner trajectories predict the size of a toner dot. If a distance between the toner particle passing through the control electrodes and the z axis is large, a toner dot obtained is big. In the opposite way, if a distance between the toner particle passing through the control electrodes and the z axis is small, then a toner dot obtained is small.

ศูนย์วิทยทรัพยากร  
จุฬาลงกรณ์มหาวิทยาลัย



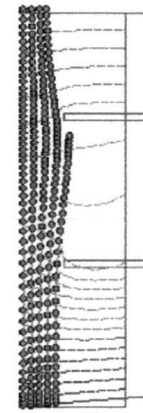
a) 0, 300, 200, 300



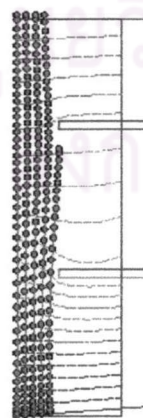
b) 0,300, 250, 350



c) 0, 300, 300, 400



d) 0,300, 350, 450



e) 0, 300, 400, 500

Figure 4-33 Toner trajectory when  $V_4-V_3 = 100 \text{ V}$

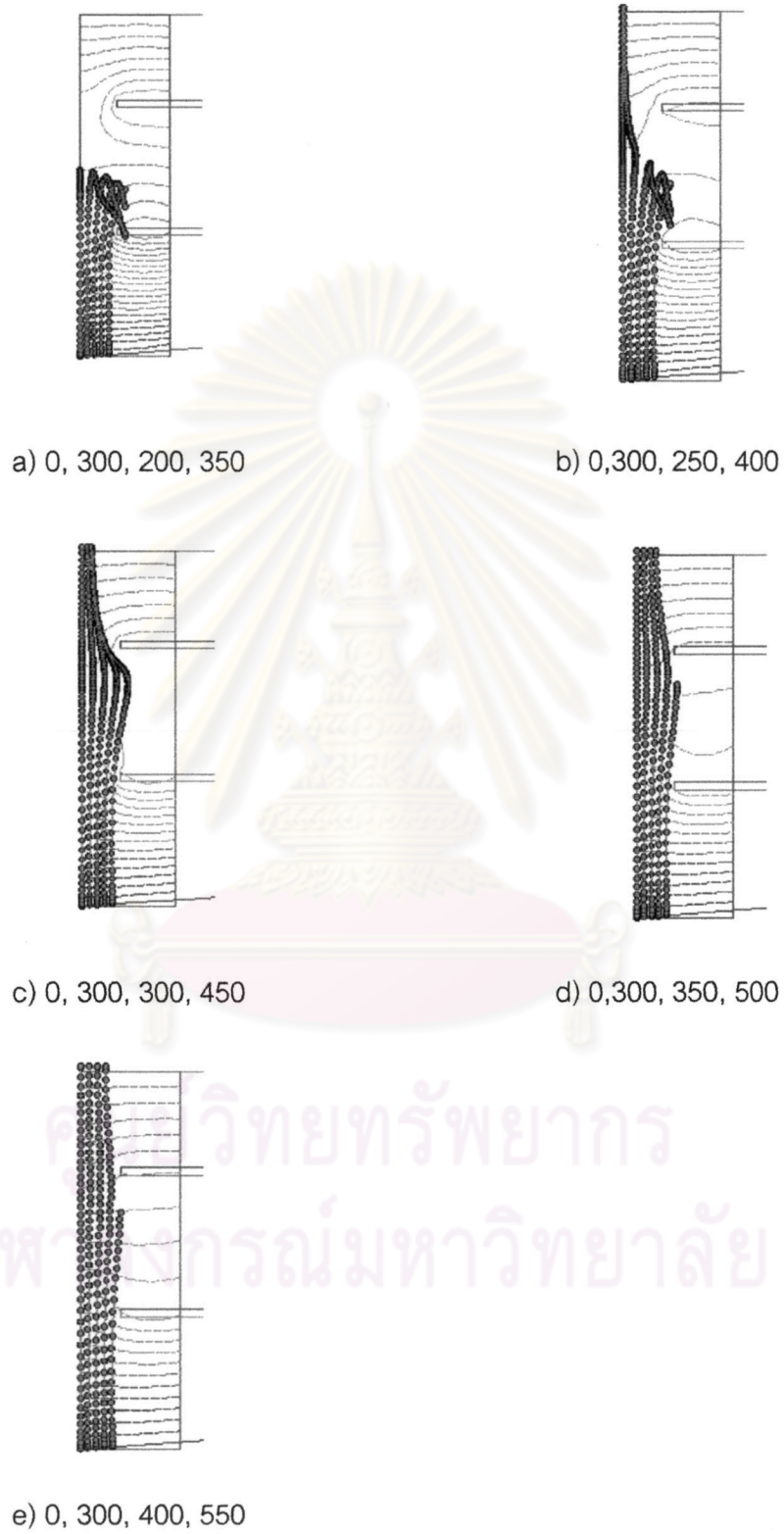


Figure 4-34 Toner trajectory when  $V_4 - V_3 = 150$  V



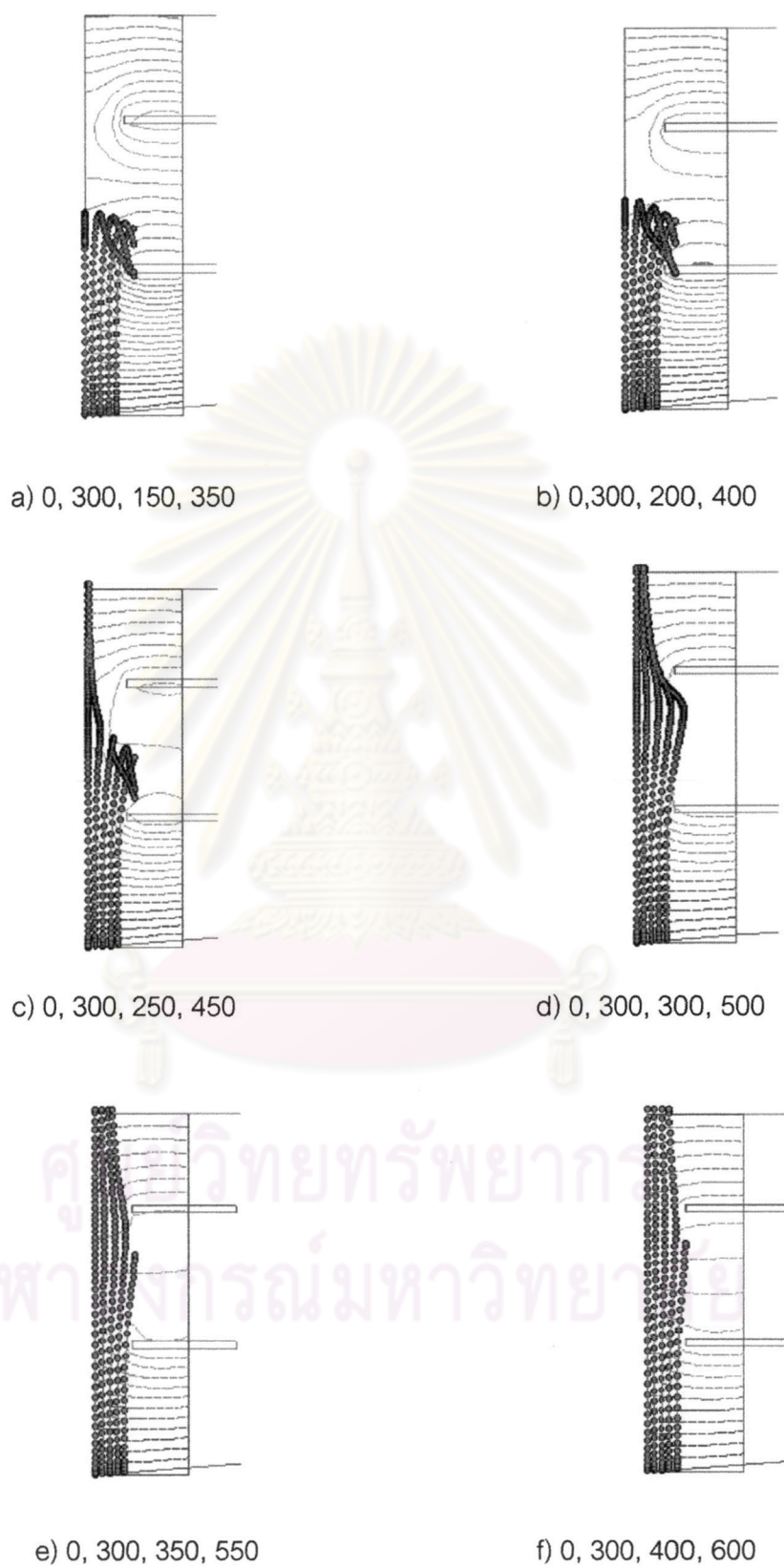


Figure 4-35 Toner trajectory when  $V_4 - V_3 = 200 \text{ V}$

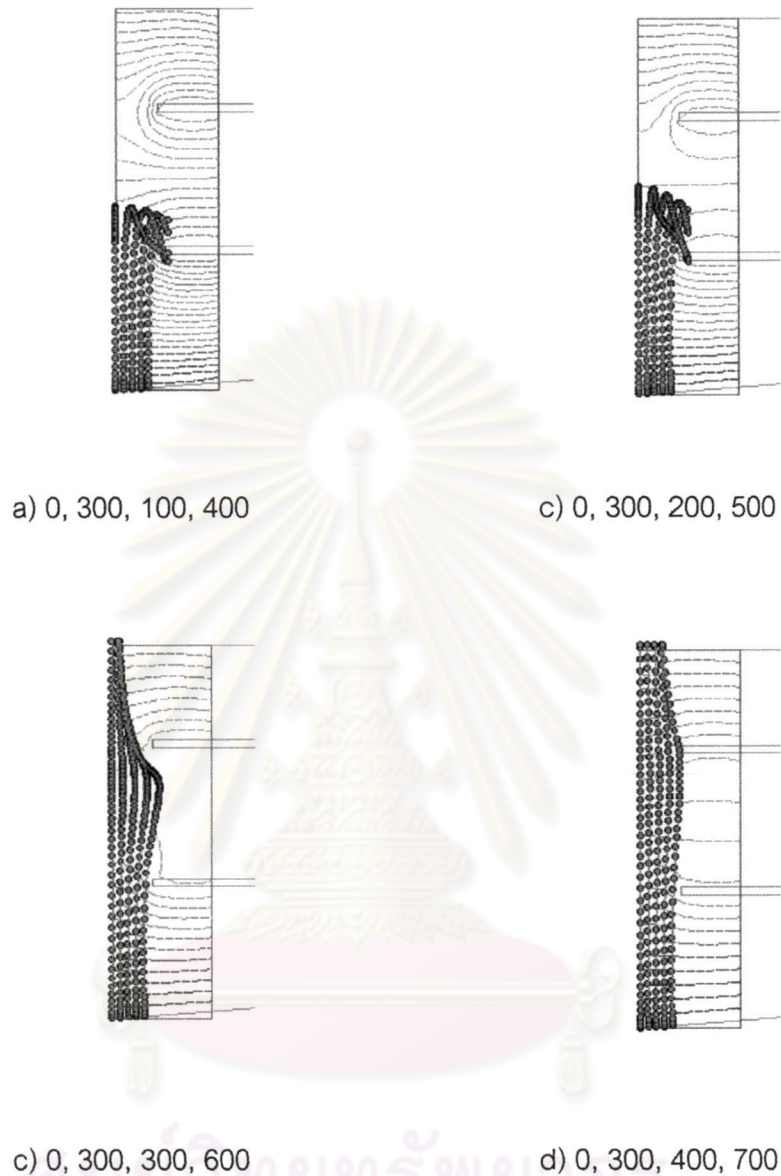


Figure 4-36 Toner trajectory when  $V_4 - V_3 = 300$  V

From the results of the simulation of toner trajectories, the beam of toner particles depends on the voltage applied to the upper control electrode. When the voltage applied to the upper control electrode is less than the voltage applied to the lower control electrode ( $V_3 < V_2$ ), the toner particles or some of them cannot pass through the control electrodes. In the other hand, when the voltage applied to the upper control electrode is more than the voltage applied the lower control electrode ( $V_3 > V_2$ ), the toner

particles can pass through the control electrodes. We can explain it by the electric field generated between the control electrodes. The electric field  $\vec{E}$  consists of the component of electric field in the x axis ( $E_x$ ), y axis ( $E_y$ ) and z axis ( $E_z$ ). Obviously,  $E_z$  affects the toner particle trajectories to move in the direction along z axis. If  $E_z$  is negative, the negatively charged particle will move up to the pulling electrode. This part is controlled by the setup of  $V_4 > V_3 > V_2 > V_1$ . When  $V_3$  is much different from  $V_2$ , the magnitude of electric field force  $E_z$  is increase in the direction of -z axis and makes the number of toner particles passed through the aperture of control electrodes increases. The experimental results from Figures 4-16 to 4-19 mostly agree qualitatively with the simulations. When the applied voltage to the upper control electrode increases, the toner dot size increases. In the other hand, if the component of the electric field along the z axis ( $E_z$ ) is positive, the negatively charged will move down to the dented electrode. This part is controlled by the setup of  $V_3 < V_2$ . The electric field generated between the control electrodes is a barrier of the toner particles and causes the toner dot size decreases. The experimental results from Figures 4-16 to 4-19 agree well with the simulation results when  $V_3 - V_2 > -50$  V. The experimental result shows that when  $V_3 - V_2 < -50$  V, the toner dot size increases, which disagrees with the simulation result. This situation is considered that, in a highly off condition, the negative toner charge is recharged at the lower control electrode and become a positive charge. These positive charges can pass through the control electrodes and some of them can reach the pulling electrode (if the electric field between the control electrodes is strong enough) as shown in Figure 4-37. Then a wider toner dot is generated.

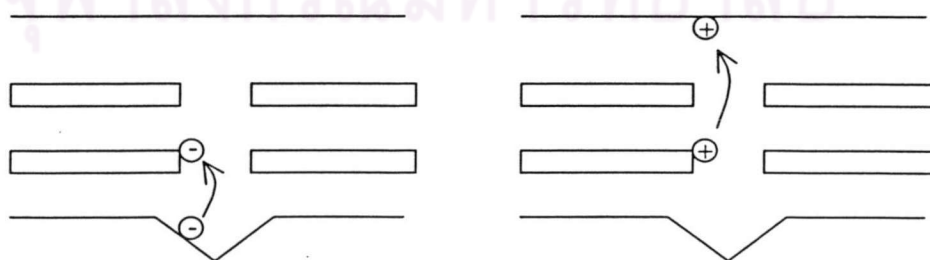


Figure 4-37 The explanation for the experimental results, which differ from the simulation results in the highly off condition

This phenomenon leads to an improvement of the aperture shape of control electrodes for the next step work. A new shape of the aperture of control electrodes as shown in Figure 4-38 is designed for preventing the contact between the toner particle and the lower control electrode.



Figure 4-38 The new shape of the aperture of control electrodes

ศูนย์วิทยทรัพยากร  
จุฬาลงกรณ์มหาวิทยาลัย